Check for updates

Received: 15 February 2023 | Revised: 23 August 2023 | Accepted: 24 August 2023

IET Communications

DOI: 10.1049/cmu2.12679

ORIGINAL RESEARCH

An intelligent age of information based self-energized UAV-assisted wireless communication system

Anandpushparaj Jeganathan[1] | **Balaji Dhayabaran**[2] | **Dushantha Nalin K. Jayakody**[3] | **Sanjaya Arunapriya Ranchagodage Don**[4] | **P. Muthuchidambaranathan**[5]

[1]Department of Electronics and Communication Engineering, SRM Institute of Science and Technology, Tiruchirappalli Campus, Tiruchirappalli, India

[2]Baseband Algorithm Development Team, Saankhya Labs Private Limited, Bengaluru, India

[3]COPELABS, Universidade de Lusofona, Lisbon, Portugal

[4]Centre for Telecommunication Research, Faculty of Postgraduate Studies & Research, Sri Lanka Technological Campus, Padukka, Sri Lanka

[5]Department of Electronics and Communication Engineering, National Institute of Technology, Tiruchirappalli, India

Correspondence
Dushantha Nalin K. Jayakody, COPELABS, Universidade de Lusofona, Lisboa, Portugal.
Email: nalin.jayakody@ieee.org

Funding information
Fundação para a Ciência e a Tecnologia, Grant/Award Numbers: (AIEE-UAV)2022.03897.PTDC, (COPELABS)UIDB/04111/2020; Ministry of Human Resource Development Scheme for Promotion of Academic and Research Collaboration (SPARC), Grant/Award Number: SPARC/2018-2019/P145/SL; COFAC - Cooperativa de Formação e Animação Cultural, Grant/Award Number: COFAC/ILIND/COPELABS/2/2022

Abstract

Internet-of-things is an enabling technology in the fourth-generation industrial revolution. The freshness of the data sent by a sensor node (SN) is an important parameter in the Internet-of-things, unlike the throughput in cellular communications. A relatively new performance metric named age of information (AoI) is used in this paper to quantify the freshness of the data. The SN, located in the transport infrastructure, harvests energy from radio frequency signals transmitted by the FD-UAV. This is used to transmit real-time sensor observations to the data sink via FD-UAV. The SN generates an update after replenishing the battery and transmits it by using the harvested energy. A closed-form expression for average AoI is derived as a function of time allocated for energy harvesting. The optimal time allocation for energy harvesting that maximizes the freshness of data update is identified. A deep learning technique namely long-short term memory is used to predict the average AoI. Simulation results demonstrate the usefulness of the performance bounds in terms of the freshness of data updates.

1 | INTRODUCTION

New innovations in fifth-generation and beyond (5GB) communication networks, particularly the Internet of things (IoT), have revolutionized a wide range of industries, including automotive, agriculture, and transportation systems. A massive number of low-power sensor nodes (SN) are positioned in fields of interest in advanced IoT applications. The freshness of the received information is critically important for IoT applications due to its value in real-time applications such as traffic control systems, command control systems etc. Thus, a unified performance metric, i.e. age of information (AoI), is introduced to capture the freshness of received data relevant to its generation time at the source. In massive IoT deployments, full-duplex (FD) communications can be used to transmit the data to the destination simultaneously while receiving it from the SN, significantly reducing the amount of time it takes for the data to be processed and analyzed. This is especially important in applications where real-time data analysis is critical, such as in healthcare or industrial settings. Additionally, FD communications can help improve network efficiency by reducing the amount of traffic on the network and minimizing the risk of packet loss or delays. Overall, FD communications are a powerful tool for ensuring that data is transmitted quickly and reliably and play a significant role in reducing the AoI.

This is an open access article under the terms of the Creative Commons Attribution-NonCommercial-NoDerivs License, which permits use and distribution in any medium, provided the original work is properly cited, the use is non-commercial and no modifications or adaptations are made.
© 2023 The Authors. *IET Communications* published by John Wiley & Sons Ltd on behalf of The Institution of Engineering and Technology.

FIGURE 1 An illustration of self-energized UAV enabled cooperative communication network in industrial Internet of things.

In addition, it is also important to provide coverage to the SNs deployed in remote places. Unmanned aerial vehicles (UAV) are identified as an effective mechanism to collect data from SNs in IoT applications, especially when there is no feasible connection to the data processing centers. Unlike traditional static data collection methods, UAV utilizes the favourable line-of-sight (LOS) dominant air-to-ground channels, increasing the coverage area.

To extend the operational life of resource-constrained IoT devices, an innovative radio frequency wireless power transfer (RF-WPT) technique was developed. RF-WPT works well in non-line-of-sight (NLOS) propagation environments as well and supports energy multicasting, making it the best candidate for powering up energy-constrained small devices in IoT applications as demosntrated in Figure 1. It has been studied for various applications in open literature, c.f. ref. [1]. A joint precoding optimization technique is introduced for secured SWIPT in UAV-aided NoMA networks in ref. [2]. Power allocation and beam forming techniques for secure communication in UAV-aided NoMA networks is proposed in ref. [3].

1.1 | Related works

The freshness of the received information is critically important for IoT applications due to its value in real-time applications such as traffic control systems, command control systems etc. Thus, a unified performance metric, i.e. age of information (AoI) is introduced to capture the freshness of received data with relevant to its generated time at the source. The AoI is technically defined as the time elapsed since the last received update packet was generated at the SN. AoI can be used to improve latency by identifying system parameters involved in latency while maintaining the expected quality of service (QoS). AoI in SWIPT-enabled wireless communication system for 5GB is presented in ref. [4]. In this work, AoI for both single-user point-to-point communication and cooperative communication along with time switching and power splitting protocol is analyzed. In refs. [5] and [6], the AAoI is modelled as the time spent by the data packets in the transmit and receive queues using queuing theory. Recent works investigated information transmission policies, which minimized the AoI performance and notion of AoI in EH-enabled communication systems [7, 8]. Contrarily, the design of EH-enabled communication systems while minimizing AoI is identified as a recent research direction with potential applications [9].

Unmanned aerial vehicle (UAV) is identified as an effective mechanism to collect data from SNs in IoT applications, especially, when there is no feasible connection towards the data processing centers. Unlike the traditional static data collection methods, UAV utilizes the favourable line-of-sight (Los) dominant air-to-ground channels increasing coverage area and sum throughput of the IoT network. However, there is a trade-off between sum throughput and energy efficiency of the system, thus, UAV should be power aware during the data collection process [10]. Furthermore, UAV's trajectory need to be optimized to maximize the number of serving IoT devices in the network while considering the performance metrics [11].

Increase in surging traffic demand in IoT applications causes a decrease in spectral efficiency due to the large amount of data introduced by the communication devices. Thus, transmission and reception simultaneously, also known as full-duplex (FD) communication long been considered to apply to IoT applications, but hindered by the self-interference (SI) from the communication device's transmitter to the receiver. In general, SI signal received from the transmitter is significantly higher than the intended received signal, making FD infeasible in practical applications [12]. However, the recent advances in analogue and digital signal processing techniques make realized the integration of FD into communication systems [13, 14].

17518636, 2023, 19, Downloaded from https://ietresearch.onlinelibrary.wiley.com/doi/10.1049/cmu2.12679, Wiley Online Library on [27/10/2026]. See the Terms and Conditions (https://onlinelibrary.wiley.com/terms-and-conditions) on Wiley Online Library for rules of use; OA articles are governed by the applicable Creative Commons License

Deep learning (DL) based approaches received great attention in recent years in many research areas including UAV applications [15]. Deep learning architectures such as a convolutional neural network (CNN), recurrent neural network (RNN), and long short-term memory (LSTM) have already been applied for UAV applications for example, attitude estimation, fault detection and target detection etc. [15–17]. The DL algorithms use multi-layered neural network architecture for mining the features in datasets from their lowest level to the highest level of training the data. It has unparalleled superiority compared to the traditional machine learning algorithm due to its feature extraction during the process of training datasets. Trained DL models can be easily deployed on the low power consuming embedded systems in order to increase the mobility of applications such as UAVs, autonomous vehicles, IOT platforms etc. [18]. With the advancement in the DL-based approaches, latency can be improved when processing mass amount of data [19–25]

Motivated by this research direction, this paper proposes a UAV-assisted wireless-powered cooperative wireless communication system to collect sensor observations from sensors to be delivered to a data sink. Then, investigate the freshness of the received information at the data sink and derived a closed-form expression for average AoI (AAoI) in the proposed system, which depends on the time allocation for EH at the SN. This work also derives a closed-form expression for AAoI, when the UAV has FD capability. It is noteworthy that this work is inspired by the commercial battery-free RF-WPT products equipped with super-capacitors, i.e. RFID sensor tags [26, 27].

1.2 | Contributions

The most significant contributions of this paper are the following:

1) An AAoI model based on the success probability of a wireless channel is presented, then a closed-form expression for AAoI in a UAV-assisted wireless powered cooperative wireless communication system is derived.
2) Investigate the effect of SI on AAoI using the proposed FD-UAV-based wireless-powered cooperative communication system.
3) This paper proves that the AAoI can be minimized by maximizing the success probability of the wireless channel. Also, note that this optimization problem is a convex optimization problem and has a global minimum.
4) A framework is built to model the proposed scheme using DL algorithms to predict AAoI with data rate and energy harvesting (EH) timing parameter (α) as the input variables as depicted in Figure 3.

This paper is organized as follows. The system model is explained in Section 2. The AAoI for the half-duplex UAV-assisted (HD-UAV) IoT and FD-UAV assisted IoT is derived in Sections 2.2 and 2.3 respectively. The deep learning algorithm for AAoI is explained in Section 3. The simulation results are provided in Section 4. Finally, the paper is concluded in Section 5.

2 | SYSTEM MODEL

2.1 | Age of information

The goal of timely updating is neither the same as maximizing the utilization of the communication system, nor of ensuring that generated status updates are received with minimum delay [28]. The performance metric that measures this timely update of information is termed as AoI.

2.1.1 | Definition

The age of information measures the time taken between the status update packet generation at the sensor node and the successful reception at the destination. In the literature, this is modelled as the waiting time of the packet in transmit and receive queues [5, 6].

AoI based on the number of re-transmissions are modelled in our work. we define the AAoI based on the time a data packet spends in the wireless channel because of re-transmissions, which primarily depends on the fading characteristics of the wireless channel. The AAoI measures the time delay between the packet generation at the SN and its successful decoding at terrestrial base station (TBS) received via FD-UAV. This paper considers a communication system architecture as illustrated in Figures 1–3, incorporating a first-come-first-served (FCFS) queuing policy with all the data packets having similar priority. The impact of the wireless channel parameters, i.e. data rate, and SI on AAoI of the proposed system is studied in detail.

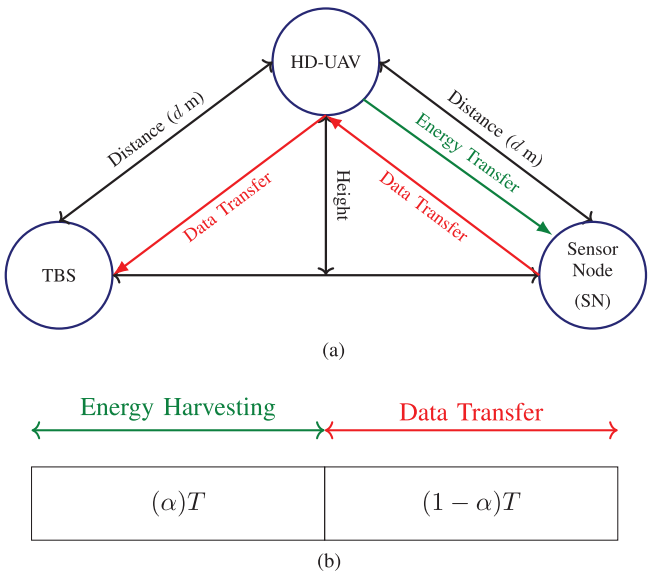

FIGURE 2 (a) HD-UAV assisted IoT- system model. (b) Energy harvesting timing diagram.

17518636, 2023, 19, Downloaded from https://ietresearch.onlinelibrary.wiley.com/doi/10.1049/cmu2.12679, Wiley Online Library on [27/10/2026]. See the Terms and Conditions (https://onlinelibrary.wiley.com/terms-and-conditions) on Wiley Online Library for rules of use; OA articles are governed by the applicable Creative Commons License

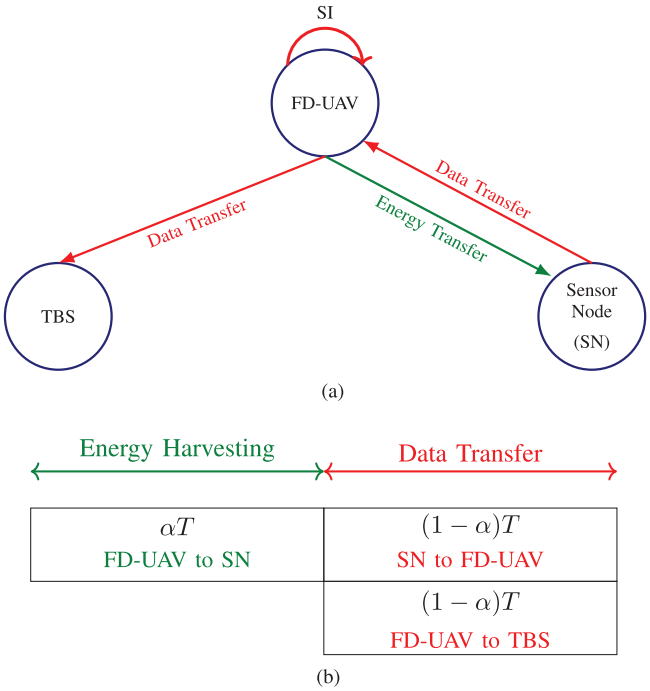

FIGURE 3 (a) FD-UAV assisted IoT - system model. (b) Energy harvesting timing diagram.

Let R denote the number of consecutive re-transmissions until successful decoding of the data packet at the UAV. The number of re-transmissions can be modelled as a geometric random variable.

$$Pr(R = r) = (1 - \Pi)^{r-1}\Pi\,, \tag{1}$$

where Π is the probability that the data packet is successfully decoded at the UAV.

The AAoI is given by

$$\text{AAoI} = \frac{1}{\Pi}. \tag{2}$$

The average time taken for a successful transmission or the freshness of data packet at the UAV is

$$F_{\text{uav}} = \frac{T}{\Pi}. \tag{3}$$

For applications like autonomous vehicles, it is very critical that the decision must be based on the data packets that are relatively fresh among all the data packets received. Thus far, it is expected that the data packets are transmitted with less number of re-transmissions. From Equation (2), it is clear that to minimize the AoI of the data packet the success probability should be maximized.

This paper considers two system models. Firstly, we consider a simple relay network as shown in Figure 2(a). The UAV used as a relay, collects information from the SN and forwards it to the TBS using decode and forward relaying technique. Assuming that the time duration of a data packet is T seconds, the SN harvests energy from the UAV for αT seconds and transmits the data packet back to the UAV in the remaining $(1-\alpha)T$ seconds as shown in Figure 2(b), where $0 < \alpha < 1$. The UAV then forwards the data packet to the TBS. In the second system model, we consider an FD-UAV as the relay. This paper models and analyzes the AAoI in both the systems described above. Further, this paper considers an urban scenario where the wireless channels between the UAV, TBS, and SN are assumed to be Rayleigh flat fading.

2.2 | AAoI in UAV-assisted IoT

The signal received by the SN from the UAV during the energy harvest slot of αT second is given by

$$Y_{\text{s}} = \alpha T\sqrt{P_{tx}}h_{\text{us}}x + W_{\text{s}}\,, \tag{4}$$

where P_{tx} is the power transmitted from the UAV for EH at the SN, h_{us} is the downlink wireless channel between the UAV and the SN, W_{s} is the additive white Gaussian noise (AWGN) with zero mean and variance σ_{s}^2, $W_{\text{s}} \sim \mathcal{N}(0, \sigma_{\text{s}}^2)$. Energy harvested in this time duration is given by,

$$E_{\text{h}} = \alpha T\eta P_{tx}h_{\text{us}}^2\,, \tag{5}$$

where η is the energy conversion efficiency. Since the envelope of the downlink channel is Rayleigh distributed, the power of the downlink channel h_{us}^2 is exponentially distributed, $h_{\text{us}}^2 \sim \exp(P_{\text{us}})$, where P_{us} is the average power of the downlink Rayleigh fading channel. From Equation (5), the average energy harvested at the SN is given as

$$E_h^{\text{avg}} = \mathbb{E}\left[\alpha T\eta P_{tx}h_{\text{us}}^2\right] = \alpha T\eta P_{tx}\mathbb{E}[h_{\text{us}}^2] \tag{6}$$

$$= \alpha T\eta P_{tx}P_{\text{us}} \tag{7}$$

where $\mathbb{E}[h_{\text{us}}^2] = P_{\text{us}}$, which denotes the average power of the Rayleigh fading downlink channel from the UAV to SN. The SN then transmits the data packet using the energy harvested from the UAV in the remaining $(1-\alpha)T$ duration. The signal-to-noise ratio (SNR) at the UAV is given as,

$$\Gamma_{\text{uav}} = \frac{E_h^{\text{avg}}h_{\text{su}}^2}{(1-\alpha)T\sigma_{\text{uav}}^2} = \frac{\alpha T\eta P_{tx}P_{\text{us}}h_{\text{su}}^2}{(1-\alpha)T\sigma_{\text{uav}}^2}$$

$$= \frac{\alpha\eta P_{tx}P_{\text{us}}h_{\text{su}}^2}{(1-\alpha)\sigma_{\text{uav}}^2}\,, \tag{8}$$

where h_{su}^2 is the power of the uplink wireless channel from the sensor node to the UAV and it is exponentially distributed $h_{\text{su}}^2 \sim \exp(P_{\text{su}})$, P_{su} is the average power of the wireless channel, and σ_{uav}^2 is the variance of the AWGN noise at the UAV.

17518636, 2023, 19, Downloaded from https://ietresearch.onlinelibrary.wiley.com/doi/10.1049/cmu2.12679, Wiley Online Library on [27/10/2026]. See the Terms and Conditions (https://onlinelibrary.wiley.com/terms-and-conditions) on Wiley Online Library for rules of use; OA articles are governed by the applicable Creative Commons License

The success Probability of the data packets transmitted at a rate r bits per second in the wireless channel between the sensor node and UAV link is given as

$$\begin{aligned}\Pi_{su} &= Pr\left[(1-\alpha)\log_2(1+\Gamma_{uav}) \geq r\right] \\ &= Pr\left(h_{su}^2 \geq \tau_{su}\right) \end{aligned} \tag{9}$$

where $\tau_{su} = \dfrac{(2^{\frac{r}{1-\alpha}}-1)(1-\alpha)\sigma^2}{\alpha\eta P_{tx} P_{us}}$.

The probability given in Equation (9) can be evaluated as,

$$\Pi_{su} = \int_{\tau_{su}}^{\infty} \left(\frac{1}{P_{su}}\right) \exp\left(\frac{-x}{P_{su}}\right) dx, \tag{10}$$

where $x = h_{su}^2$. The success probability obtained by solving the integral in Equation (10) is,

$$\Pi_{su} = \exp\left(\frac{-\tau_{su}}{P_{su}}\right) \tag{11}$$

Similarly the success probability of the UAV to TBS link can be written as,

$$\Pi_{ut} = \exp\left(\frac{-\tau_{ut}}{P_{ut}}\right), \tag{12}$$

where $\tau_{ut} = (2^r - 1)\sigma_{tbs}^2 / P_{uav}$, σ_{tbs}^2 is the variance of the AWGN noise at TBS, P_{uav} is the transmit power at the UAV, and P_{ut} is the average power of the wireless channel between the UAV and the TBS. The overall success probability of the link between the sensor node to TBS is the product of the two success probabilities given in Equations (11) and (12).

$$\begin{aligned}\Pi &= \Pi_{su}\Pi_{ut} \\ &= \exp\left(\frac{-\tau_{su}}{P_{su}} + \frac{-\tau_{ut}}{P_{ut}}\right) \end{aligned} \tag{13}$$

The objective is to maximize this success probability in order to minimize the AAoI.

$$\begin{aligned} \max_{\alpha} \quad & \exp\left(\frac{-\tau_{su}}{P_{su}} + \frac{-\tau_{ut}}{P_{ut}}\right) \\ \text{subject to} \quad & 0 < \alpha < 1 \end{aligned} \tag{14}$$

Substituting the value of τ_{su} and τ_{ut}, (14) can be written as,

$$f(\alpha) = \exp\left(\frac{-(2^{\frac{r}{1-\alpha}}-1)(1-\alpha)\sigma^2}{\alpha\eta P_{tx} P_{us} P_{su}} - \frac{(2^r-1)\sigma_{tbs}^2}{P_{uav} P_{ut}}\right)$$

Using the logarithm of the objective function, the optimization problem in Equation (14) can be simplified as,

$$\begin{aligned} \min_{\alpha} \quad & \frac{\left(2^{\frac{r}{1-\alpha}}-1\right)(1-\alpha)}{\alpha} \\ \text{subject to} \quad & 0 < \alpha < 1 \end{aligned} \tag{15}$$

Lemma 1. *The optimization problem given in Equation (15) is a convex optimization problem and has a global minimum.*

Proof. The proof is provided in Appendix A. □

2.3 | AoI in full-duplex UAV-assisted IoT

In this system model, we use an FD-UAV as a relay unlike the previous system, where we used HD-UAV as a relay. The SI at the FD-UAV along with the EH time ratio α plays an important role in the AAoI of this system.

The SN generates a real-time status update data packet and then transmits to the TBS through an FD-UAV. The receivers (FD-UAV, and TBS) will request for re-transmission upon erroneous decoding of the data packet. As the number of re-transmissions increases, the AAoI also increases. The signal-to-interference plus noise ratio (SINR) at the UAV is given as

$$\Gamma_{\text{fd-uav}} = \frac{\alpha\eta P_{tx} P_{us} h_{su}^2}{(1-\alpha)\sigma_{uav}^2 + P_{si}}, \tag{16}$$

where P_{si} is the SI power. The success probability of the end-to-end link from SN to TBS through FD-UAV is given as,

$$\Pi = \exp\left(\frac{-\tau_{su}}{P_{su}} + \frac{-\tau_{ut}}{P_{ut}}\right), \tag{17}$$

where

$$\tau_{su} = \frac{(2^{\frac{r}{1-\alpha}}-1)(1-\alpha)\left(\sigma_{uav}^2 + P_{si}\right)}{\alpha\eta P_{tx} P_{us}},$$

$$\tau_{ut} = \frac{\left(2^{\frac{r}{1-\alpha}}-1\right)\sigma_{tbs}^2}{P_{uav}}$$

σ_{uav}^2, and σ_{tbs}^2 are the additive white Gaussian noise at the UAV and TBS respectively. The AAoI is calculated using Equation (2).

3 | DL BASED AAOI PREDICTION MODEL

The LSTM algorithm is mainly constructed with a long chain of repeating memory units called memory cells. The cell state is

17518636, 2023, 19, Downloaded from https://ietresearch.onlinelibrary.wiley.com/doi/10.1049/cmu2.12679, Wiley Online Library on [27/10/2026]. See the Terms and Conditions (https://onlinelibrary.wiley.com/terms-and-conditions) on Wiley Online Library for rules of use; OA articles are governed by the applicable Creative Commons License

a small buffer that passes into each memory cell by the LSTM chain. When the cell state passes between the memory cells, the content is modified using logic states namely, "forget logic" and "input logic." In the initialization, the LSTM decides the information to be passed away from the cell state by a sigmoid layer. It checks the previous state and current input of the memory cell and turns out the logic state between 0 and 1 for each number in the cell state. If the output is 1, content is retained for carrying out the predictions and if the output is 0, the content is modified.

The memory cells of the LSTM algorithm are mainly functioned by three gates namely, "the input gate," "the forgetting gate," and "the output gate." The input gate enables the input of information of the memory cell and the forgetting gate selectively eliminates some information in the memory cell and enables the buffer to the next input. Finally, the output gate decides on the information to be outputted by the memory cell.

The LSTM starts its recognition procedure with an input sequence $x = (r, \alpha, k)$ and finally outputs $y = (\text{AAoI})$ which is calculated as follows. RNN is a deep learning algorithm that has a high capability for capturing the hidden inter-dependencies in image captioning, voice conversion, and natural language processing etc. LSTM is an improved version of RNN which contains a special structure of the hidden layers compared to that of the RNN structures. The LSTM algorithm has already been successfully applied for UAV applications such as altitude estimation, fault detection, target detection etc.

$$i_n = \sigma(W_{ix}x_i + W_{im}m_{n-1} + b_i) \tag{18}$$

$$o_n = \sigma(W_{ox}x_n + W_{om}m_n + b_o) \tag{19}$$

$$f_n = (1 - i_n) \tag{20}$$

$$z_n = g(W_{cx}x_n + W_{cm}m_{n-1} + b_c) \tag{21}$$

$$c_n = f_n \odot c_{n-1} + i_n \odot z_n \tag{22}$$

$$m_n = o_n \odot hc_n \tag{23}$$

$$y_n = \phi(W_{ym}m_n + b_y) \tag{24}$$

In these equations, i, o, and f mean the input gate, output gate and forget gate. z is the input information to the memory cell, σ is the sigmoid function, and, c and m are the cell activation vector and the information of the output of the memory cell respectively. Weight matrices are represented by the W. The bias vector is represented as b where b_i is the input gate bias vector. g and h represent the cell input activation functions and the cell output activation functions respectively which are considered to be considered to be tan$h$ functions. $\odot$ is the point multiplication in a matrix. ϕ is the activation function of the neural network output.

AAoI is predicted by introducing a trained model, based on LSTM algorithm, the working procedure of the trained model is illustrated in Figure 4. In this model, the nonlinear relationship between r, α, and AAoI are trained based on the data retrieved from the mathematical simulation results on Equation (7). As a result, a trained model that predicts the AAoI values prior to any change of r and α.

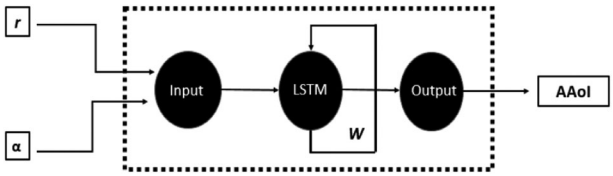

FIGURE 4 LSTM model for predicting the AAoI.

The mean squared error (MSE) defines the difference between the model-predicted AAoI values and the actual AAoI values. The performance of the model in predicting the AAoI values is evaluated by the MSE. When the MSE is small, it gives higher prediction accuracy and is calculated as

$$\text{MSE} = \frac{1}{N}\sum_{i=1}^{N}\left(\text{AAoI} - \overline{\text{AAoI}}\right) \tag{25}$$

where AAoI is the actual value and $\overline{\text{AAoI}}$ is the estimation. Simulation experiments are carried out to determine the performance of the DL model. For improving the accuracy of the model, the parameters of the model are selected carefully, i.e. the number of iterations (epochs) and the number of neurons in the hidden layer.

4 | RESULTS AND DISCUSSIONS

In this section, simulation results are presented to identify the performance bounds of the proposed system. We assume that the noise power at both UAV and the TBS are equal. Unless otherwise stated, we set the values for simulation parameters as follows. The EH efficiency at the SN is set to $\eta = 0.9$, time slot duration is $T = 1$ s, the transmit power of the UAV during the EH phase is set as 37 dBm and during the information transfer to the AP is 30 dBm. We assume that the residual SI power after performing digital SI cancellation is proportional to the noise power at the UAV given as $K\sigma^2_{\text{uav}}$, where $K = \{1, 2, 3\}$ denotes the residual SI ratio proportional to the noise power.

4.1 | Impact of time ratio (α) & information rate on AAoI

In Figure 5, the AAoI as function of time split parameter α is plotted for different values of data rates $r = \{0.5, 1, 1.5, 2\}$. The AAoI attains its maximum for smaller and larger values of α. For smaller values of α, the SN gets only less time to harvest energy resulting in less power to transmit information, thus, the AAoI increases. For larger values of α, the SN gets enough time to harvest energy, but less time to transmit information, causing an increase in AAoI in fixed. It is also observed from this

17518636, 2023, 19, Downloaded from https://ietresearch.onlinelibrary.wiley.com/doi/10.1049/cmu2.12679, Wiley Online Library on [27/10/2026]. See the Terms and Conditions (https://onlinelibrary.wiley.com/terms-and-conditions) on Wiley Online Library for rules of use; OA articles are governed by the applicable Creative Commons License

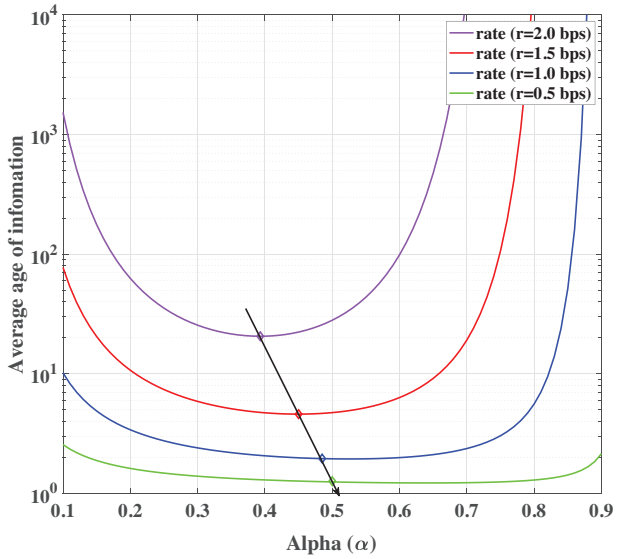

FIGURE 5 AAoI versus α for rate, $r = \{0.5, 1, 1.5, 2\}$.

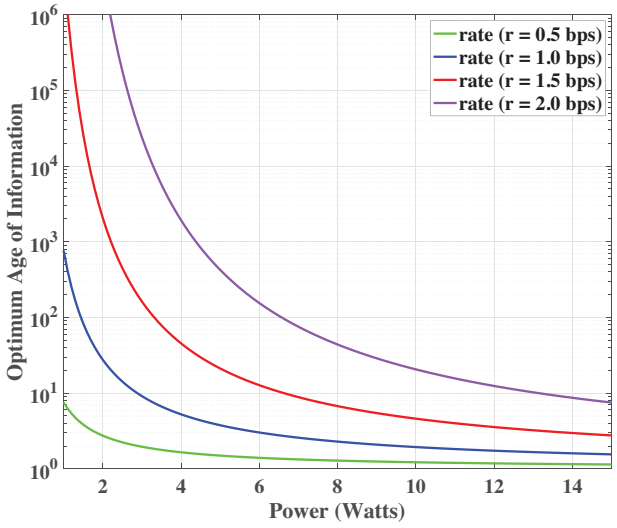

FIGURE 6 Minimum AAoI versus transmit power for rate, $r = \{0.5, 1, 1.5, 2\}$.

figure that the increase in data rate causes an increase in AAoI. This observation makes sense since the increase in data date causes an increase in error probability for a fixed value of α. Thus, the number of re-transmission of data packet rise up causing an increase in the AAoI of the system. It is noteworthy that the polygons inside Figure 5 show the optimal values of AAoI. Since AAoI is a convex function with respect to α, the local optimum value is also can be considered as the global optimum.

4.2 | Impact of the UAV's transmission power & information rate on AAoI

The SN uses the energy harvested from the UAV to transmit the data packet. Clearly, the AAoI depends on the energy harvested by the SN, which also depends on the transmit power of the UAV during the EH phase. The dependence of AAoI on the transmit power of the UAV is represented in Figure 6. The optimal values for time ratio α obtained in Figure 5 is used in this simulation. It can be noticed from the Figure 6 that as the transmit power of the UAV increases the AoI decreases. In addition, it can also be noticed from the figure that the AoI decreases linearly in the low-power region and it reaches a constant value of 1 at the high-power region. This can be understood mathematically using the polynomial expansion of AAoI, which is an exponential function. In the high power region, the higher order terms in the polynomial expansion will cancel out and the AAoI can be approximated as 1. It is also logical that the minimum value of AoI is 1 as the data packet has to be transmitted at least once for successful decoding at the receiver.

4.3 | Impact of the height of UAV on AAoI

As shown in the system model the UAV flies at a height of h m above the ground. The distance of separation between the

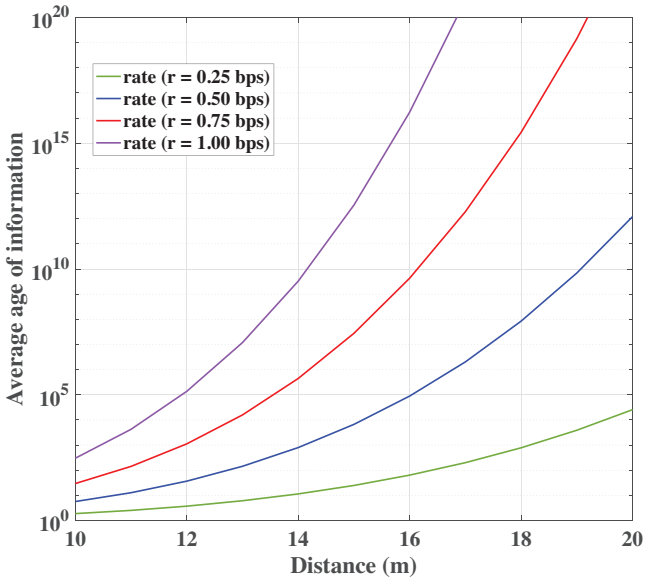

FIGURE 7 Minimum AAoI versus distance for rate, $r = \{0.25, 0.5, 0.75, 1\}$.

UAV, TBS, and SN also plays an important role in AAoI. As the height of the UAV increases the distance between UAV and the other two nodes also increases. This results in an increase in the path loss as well which in turn results in poor AAoI. This characteristic of AAoI is shown in Figure 7. For this analysis, we assume that the UAV is located halfway between the TBS and SN at a height of h m, and the distance of separation between the UAV, TBS, and SN are d m as shown in Figure 2(a). From the figure, it can be observed that as the distance increases the AAoI increases exponentially for different data rates. Transmission techniques like power allocation, beamforming, receiver algorithms, and UAV trajectory optimization [29] can be used to optimize AAoI in this scenario.

17518636, 2023, 19, Downloaded from https://ietresearch.onlinelibrary.wiley.com/doi/10.1049/cmu2.12679, Wiley Online Library on [27/10/2026]. See the Terms and Conditions (https://onlinelibrary.wiley.com/terms-and-conditions) on Wiley Online Library for rules of use; OA articles are governed by the applicable Creative Commons License

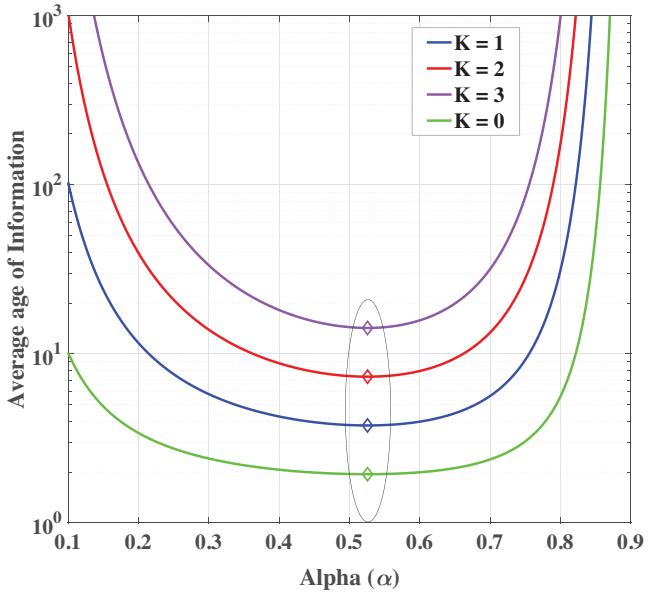

FIGURE 8 AAoI versus α for $K = \{0, 1, 2, 3\}$.

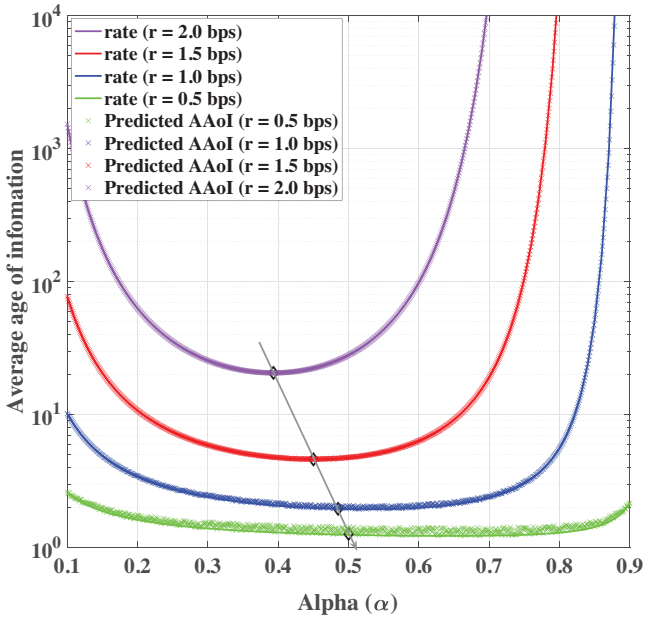

FIGURE 9 Comparison of actual AAoI with AAoI predicted by DL algorithm versus α for rate, $r = \{0.5, 1, 1.5, 2\}$.

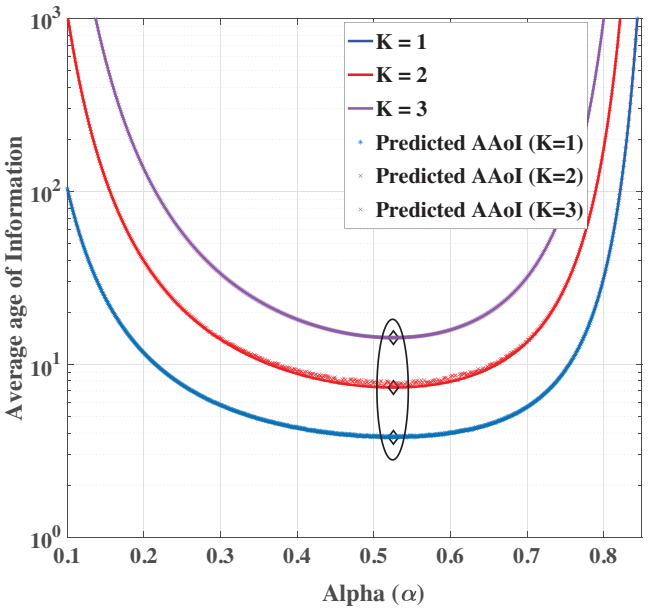

FIGURE 10 Comparison of actual AAoI with AAoI predicted by the DL algorithm versus α for $K = \{1, 2, 3\}$.

4.4 | Impact of the SI & time ratio (α) on AAoI

Another major factor that affects AoI, especially in an FD system is the SI. Though there are many SI cancellation schemes available in the open literature, a small residual interference will adversely affect the received signal at the UAV. The impact of SI on AAoI is shown in Figure 8. We compare the effect of different magnitudes of SI power over the AAoI of the system with the ideal case where it is assumed that a genie-aided SI cancellation technique completely cancels out the SI power. It can be clearly seen from the Figure 8 that $K = 0$ denotes the ideal case where SI power is zero. For this simulation, the r is kept constant in the value of 0.5. As the SI power increases the SINR at the UAV (Γ_{su}) decreases affecting the probability of successful transmission. Thus, it can be seen from the figure that as the SI power increases the AoI also increases. The polygons in Figure 8 represent the optimum value of α, which minimizes the AAoI regardless of the SI. Since the AAoI is a convex function, the local minimum of α is also can consider as the global minimum.

4.5 | Performance of LSTM model

The LSTM model was implemented on Tensor flow 2.0 with the Python and Keras deep learning frameworks. The experiment is carried out in a computer with a 16 GB RAM and i5 CPU with 2.8 GHz processor. In order to ensure the accuracy of the experiment, the training data to the model is obtained from Equation (2).

The mathematical simulation results obtained for half duplex and full duplex scenarios which were considered as actual values and the model estimated values of AAoI are shown in Figures 9 and 10 respectively. An accuracy of 90% is achieved from the LSTM model. The accuracy can be further improved by increasing the number of training epochs, size of training data set and number of neurons, which demands longer training duration.

5 | CONCLUSION

This paper proposes a UAV-assisted wireless-powered cooperative wireless communication system to collect sensor observations from sensors to be delivered to a TBS. AAoI is modelled

17518636, 2023, 19, Downloaded from https://ietresearch.onlinelibrary.wiley.com/doi/10.1049/cmu2.12679, Wiley Online Library on [27/10/2026]. See the Terms and Conditions (https://onlinelibrary.wiley.com/terms-and-conditions) on Wiley Online Library for rules of use; OA articles are governed by the applicable Creative Commons License

based on the number of retransmissions in the wireless channel. A closed-form expression for AAoI is derived for the proposed system. This depends on the success probability of the wireless channel and the time allocation for the EH at the SN. An optimization problem is formulated to evaluate the optimum value of α by minimizing the AAoI for both full-duplex and half-duplex case. As the transmit power of the UAV increases, the energy harvested by the SN increases, thus reducing the AAoI. It is shown through the simulation result that in the low-power region, AAoI reduces exponentially and it reaches a minimum value of 1 in the high-power region. The effect of SI over the AAoI is also analyzed. From the simulation results it is shown that the AAoI increases with the increase in SI. Furthermore, a deep learning algorithm, namely LSTM algorithm is used to predict the AAoI and it attains an accuracy of 90%. This DL model can be adopted to implement another AAoI-based communication system through the transfer learning process in the future.

AUTHOR CONTRIBUTIONS

Anand P: Investigation, methodology, software. Balaji D: Formal analysis, investigation, methodology, resources, software, writing - original draft. DUSHANTHA NALIN K. JAYAKODY: Conceptualization, funding acquisition, investigation, methodology, project administration, resources, supervision, visualization, writing - review and editing. Arunapriya R D S: Data curation, software, validation, visualization, writing - original draft. Muthuchidambaranathan P: Conceptualization, funding acquisition, project administration, resources, supervision.

ACKNOWLEDGMENTS

This work was funded, in part, by the COFAC - Cooperativa de Formação e Animação Cultural, C.R.L.(University of Lusófona), via the Grant No.: COFAC/ILIND/COPELABS/2/2022, by national funds through FCT - Fundação para a Ciência e a Tecnologia - as part the Project - No. 2022.03897.PTDC and grant No .: UIDB / 04111/2020 (COPELABS) and Scheme for Promotion of Academic and Research Collaboration (SPARC), Ministry of Human Resource Development, India No. SPARC/2018-2019/P145/SL.

CONFLICT OF INTEREST

The authors declare no conflict of interest.

DATA AVAILABILITY STATEMENT

Data sharing is not applicable to this article as no new data were created or analyzed in this study.

ORCID

Dushantha Nalin K. Jayakody https://orcid.org/0000-0002-7004-2930

REFERENCES

1. Jayakody, D.N.K., Perera, T.D.P., Ghrayeb, A., Hasna, M.O.: Self-energized UAV-assisted scheme for cooperative wireless relay networks. IEEE Trans. Veh. Technol. 69(1), 578–592 (2020)
2. Wang, W., Tang, J., Zhao, N., Liu, X., Zhang, X.Y., Chen, Y., Qian, Y.: Joint precoding optimization for secure SWIPT in UAV-aided NOMA networks. IEEE Trans. Commun. 68(8), 5028–5040 (2020)
3. Zhao, N., Li, Y., Zhang, S., Chen, Y., Lu, W., Wang, J., Wang, X.: Security enhancement for NOMA-UAV networks. IEEE Trans. Veh. Technol. 69(4), 3994–4005 (2020)
4. Perera, T.D.P., Jayakody, D.N.K., Pitas, I., Garg, S.: Age of information in SWIPT-enabled wireless communication system for 5GB. IEEE Wireless Commun. 27(5), 162–167 (2020)
5. Costa, M., Codreanu, M., Ephremides, A.: On the age of information in status update systems with packet management. IEEE Trans. Inf. Theory 62(4), 1897–1910 (2016)
6. Sun, Y., Uysal-Biyikoglu, E., Yates, R.D., Koksal, C.E., Shroff, N.B.: Update or wait: how to keep your data fresh. IEEE Trans. Inf. Theory 63(11), 7492–7508 (2017)
7. Arafa, A., Yang, J., Ulukus, S., Poor, H.V.: Age-minimal transmission for energy harvesting sensors with finite batteries: online policies. IEEE Trans. Inf. Theory 66(1), 534–556 (2020)
8. Wu, X., Yang, J., Wu, J.: Optimal status update for age of information minimization with an energy harvesting source. IEEE Trans. Green Commun. Networking 2(1), 193–204 (2018)
9. Krikidis, I.: Average age of information in wireless powered sensor networks. IEEE Wireless Commun. Lett. 8(2), 628–631 (2019)
10. Lin, X., Su, G., Chen, B., Wang, H., Dai, M.: Striking a balance between system throughput and energy efficiency for UAV-IoT systems. IEEE Internet Things J. 6(6), 10519–10533 (2019)
11. Samir, M., Sharafeddine, S., Assi, C.M., Nguyen, T.M., Ghrayeb, A.: UAV trajectory planning for data collection from time-constrained IoT devices. IEEE Trans. Wireless Commun. 19(1), 34–46 (2020)
12. Mobini, Z., Mohammadi, M., Chalise, B.K., Suraweera, H.A., Ding, Z.: Beamforming design and performance analysis of full-duplex cooperative NOMA systems. IEEE Trans. Wireless Commun. 18(6), 3295–3311 (2019)
13. Sun, L., Li, Y., Zhang, Z., Feng, Z.: Compact co-horizontally polarized full-duplex antenna with omnidirectional patterns. IEEE Antennas Wireless Propag. Lett. 18(6), 1154–1158 (2019)
14. Mohammadi, M., Shi, X., Chalise, B.K., Ding, Z., Suraweera, H.A., Zhong, C., Thompson, J.S.: Full-duplex non-orthogonal multiple access for next generation wireless systems. IEEE Commun. Mag. 57(5), 110–116 (2019)
15. Wang, B., Peng, X., Jiang, M., Liu, D.: Real time fault detection for UAV based on model acceleration engine. IEEE Trans. Instrum. Meas. 69(12), 9505–9516 (2020)
16. Furusho Becker, Y.V., Lopes Siqueira, H., Matsubara, E.T., Nunes Gonçalves, W., Marcato, J.M.: Asphalt pothole detection in UAV images using convolutional neural networks. In: IGARSS 2019-2019 IEEE International Geoscience and Remote Sensing Symposium, pp. 56–58. IEEE, Piscataway, NJ (2019)
17. Liu, Y., Zhou, Y., Li, X.: Attitude estimation of unmanned aerial vehicle based on LSTM neural network. In: 2018 International Joint Conference on Neural Networks (IJCNN), pp. 1–6. IEEE, Piscataway, NJ (2018)
18. Xu, J., Wang, B., Li, J., Hu, C., Pan, J.: Deep learning application based on embedded GPU. In: 2017 First International Conference on Electronics Instrumentation Information Systems (EIIS), pp. 1–4. IEEE, Piscataway, NJ (2017)
19. Meena, G., Sharma, D., Mahrishi, M.: Traffic prediction for intelligent transportation system using machine learning. In: 2020 3rd International Conference on Emerging Technologies in Computer Engineering: Machine Learning and Internet of Things (ICETCE), pp. 145–148. IEEE, Piscataway, NJ (2020)
20. Liao, Y., Friderikos, V.: Energy and age pareto optimal trajectories in uav-assisted wireless data collection. IEEE Trans. Veh. Technol. 71(8), 9101–9106 (2022)
21. Liu, J., Tong, P., Wang, X., Bai, B., Dai, H.: UAV-aided data collection for information freshness in wireless sensor networks. IEEE Trans. Wireless Commun. 20(4), 2368–2382 (2021)
22. Abd-Elmagid, M.A., Dhillon, H.S.: Average peak age-of-information minimization in UAV-assisted IoT networks. IEEE Trans. Veh. Technol. 68(2), 2003–2008 (2019)

17518636, 2023, 19, Downloaded from https://ietresearch.onlinelibrary.wiley.com/doi/10.1049/cmu2.12679, Wiley Online Library on [27/10/2026]. See the Terms and Conditions (https://onlinelibrary.wiley.com/terms-and-conditions) on Wiley Online Library for rules of use; OA articles are governed by the applicable Creative Commons License

23. Basnayaka, C.M.W., Jayakody, D.N.K., Chang, Z.: Age-of-information-based URLLC-enabled UAV wireless communications system. IEEE Internet Things J. 9(12), 10212–10223 (2022)
24. Han, R., Wang, J., Bai, L., Liu, J., Choi, J.: Age of information and performance analysis for UAV-aided IoT systems. IEEE Internet Things J. 8(19), 14447–14457 (2021)
25. Jeganathan, A., Dhayabaran, B., Perera, T.D.P., Jayakody, D.N.K., Muthuchidambaranathan, P.: Harvest-on-sky: an AOI-driven UAV-assisted wireless communication system. IEEE Internet of Things Magazine 5(1), 142–146 (2022)
26. Powercast Corporation 2020: Wireless power for wireless world. https://www.powercastco.com/ourproducts/ (2020). Accessed 15 May 2020
27. e-peas-semiconductors 2020: RF energy harvesting solutions. https://e-peas.com/types/energy-harvesting/rf/ (2020). Accessed 15 May 2020
28. Kaul, S., Yates, R., Gruteser, M.: Real-time status: how often should one update? In: 2012 Proceedings IEEE INFOCOM, pp. 2731–2735. IEEE, Piscataway, NJ (2012)
29. Yeh, S., Wang, Y., Perera, T.D.P., Peter Hong, Y., Jayakody, D.N.K.: UAV trajectory optimization for data-gathering from backscattering sensor networks. In: ICC 2020-2020 IEEE International Conference on Communications (ICC), pp. 1–6. IEEE, Piscataway, NJ (2020)

How to cite this article: Jeganathan, A., Dhayabaran, B., Jayakody, D.N.K., Don, S.A.R., Muthuchidambaranathan, P.: An intelligent age of information based self-energized UAV-assisted wireless communication system. IET Commun. 17, 2141–2151 (2023). https://doi.org/10.1049/cmu2.12679

APPENDIX A: PROOF OF EXISTENCE OF GLOBAL MINIMUM

Reiterating the AAoI optimization problem in Equation (15), we have

$$\begin{aligned} \min_{\alpha} \quad & f(\alpha) = \frac{\left(2^{\frac{r}{1-\alpha}} - 1\right)(1-\alpha)}{\alpha} \\ \text{subject to} \quad & 0 < \alpha < 1 \end{aligned} \tag{A.1}$$

The optimization problem is over the open interval $\alpha \in (0, 1)$. Hence it is necessary to prove that the minimum exists. Since this is a single variable function, the minimum point can be obtained by equating the first-order derivative to zero. The first-order derivative of the objective function is given as

$$f'(\alpha) = \frac{2^{\frac{r}{1-\alpha}}\left(\alpha(1 + r\ln(2)) - 1\right) + (1-\alpha)}{(1-\alpha)\alpha^2} \tag{A.2}$$

First, we show that the objective function $f(\alpha)$ is monotonically increasing in an interval $[x, 1)$, i.e. if we consider an interval $a < c < b$, the function $f(\alpha)$ is strictly increasing in $[c, b)$. This can be proved by showing that $f'(\alpha)$ is greater than zero in the interval $[c, b)$. From Equation (A.2), we can show that $f'(\alpha) > 0$, when the following condition is satisfied.

$$\begin{aligned} \left(\alpha(1 + r\ln(2)) - 1\right) - 1 > 0 \\ \alpha > \frac{1}{1 + r\ln(2)} \end{aligned} \tag{A.3}$$

From Equation (A.3) it is clear that $f(\alpha)$ is strictly increasing in the interval $[1/(1 + r\ln(2)), 1)$. Similarly, it can be inferred that the function is either strictly decreasing or remains constant in the interval $(0, 1/(1 + r\ln(2))]$. It can also be inferred that $f(\alpha)$ do not attain its minimum at $\alpha = 1/(1 + r\ln(2))$, which can be confirmed from the fact that

$$f'\left(\frac{1}{1 + r\ln(2)}\right) \neq 0 \tag{A.4}$$

From Equation (A.4), and from the observation that the function is strictly increasing in the interval $[1/(1 + r\ln(2)), 1)$, it can be concluded that, if at all a minimum exists for the function $f(\alpha)$ it exists in the interval $(0, 1/(1 + r\ln(2))]$.

Now our objective is to prove that $f'(\alpha)$ takes a value of zero at least once in the interval $(0, 1/(1 + r\ln(2))]$. The derivative of the objective function $f'(\alpha)$ is a continuous function in the interval $(0, 1/(1 + r\ln(2))]$. Using Equations (A.2) and (A.3), we can write

$$\begin{aligned} f'\left(\frac{1}{r\ln(2)}\right) > 0 \\ \lim_{\alpha \to 0} f'(\alpha) = -\infty. \end{aligned} \tag{A.5}$$

According to intermediate value theorem for continuous functions and using Equation (A.5) it can be concluded that there is at least one value c in the interval $0 < c < 1/(1 + r\ln(2)))$ such that $f'(c) = 0$ and the corresponding $f(c)$ is either a global or local minimum of our objective function. If the objective function is a convex function, $f(c)$ will be the global minimum. We rewrite the objective function as,

$$f(\alpha) = f_1(\alpha) f_2(\alpha) = \left(2^{\frac{r}{1-\alpha}}\right)\frac{(1-\alpha)}{\alpha}, \tag{A.6}$$

where $f_1(\alpha) = (2^{\frac{r}{1-\alpha}})$, and $f_2(\alpha) = (1-\alpha)/\alpha$.

The first order and second order derivatives of $f_1(\alpha)$ is given as

$$\begin{aligned} f_1'(\alpha) &= \left(2^{\frac{r}{1-\alpha}}\right)\frac{r\ln(2)}{(1-\alpha)^2} \\ f_1''(\alpha) &= \frac{\ln^2(2) r^2 \cdot 2^{\frac{r}{1-\alpha}}}{(1-\alpha)^2(\alpha-1)^2} + \frac{\ln(2) r \cdot 2^{\frac{r}{1-\alpha}+1}}{(1-\alpha)^3} \end{aligned} \tag{A.7}$$

Similarly the derivatives of $f_2(\alpha)$ is given as

$$\begin{aligned} f_2'(\alpha) &= \frac{-1}{\alpha^2} \\ f_2''(\alpha) &= \frac{2}{\alpha^3} \end{aligned} \tag{A.8}$$

17518636, 2023, 19, Downloaded from https://ietresearch.onlinelibrary.wiley.com/doi/10.1049/cmu2.12679, Wiley Online Library on [27/10/2026]. See the Terms and Conditions (https://onlinelibrary.wiley.com/terms-and-conditions) on Wiley Online Library for rules of use; OA articles are governed by the applicable Creative Commons License

The necessary and sufficient condition for a function $f(\alpha)$ to be convex is

$$f''(\alpha) \geq 0$$

$$f''(\alpha) = \frac{d^2}{d\alpha^2} f(\alpha) = \frac{d^2}{d\alpha^2}\left(f_1(\alpha) f_2(\alpha)\right) \geq 0$$

$$= f_2(\alpha) f_1''(\alpha) + 2 f_1'(\alpha) f_2'(\alpha) + f_1(\alpha) f_2''(\alpha) \geq 0 \tag{A.9}$$

Substituting Equations (A.7) and (A.8) in Equation (A.9), we see that $f''(\alpha) \geq 0$. Thus it is clear that $f(\alpha)$ is a convex function and the minimum of this function is the global minimum.

17518636, 2023, 19, Downloaded from https://ietresearch.onlinelibrary.wiley.com/doi/10.1049/cmu2.12679, Wiley Online Library on [27/10/2026]. See the Terms and Conditions (https://onlinelibrary.wiley.com/terms-and-conditions) on Wiley Online Library for rules of use; OA articles are governed by the applicable Creative Commons License